Clean Technologies and Environmental Policy
https://doi.org/10.1007/s10098-023-02581-5

ORIGINAL PAPER

The utilization of bio-ethanol for production of 1-butanol catalysed by Mg–Al mixed metal oxides enhanced by Cu or Co

Karel Frolich[1] · Jan Malina[1] · Martin Hájek[1] · Jáchym Mück[1] · Jaroslav Kocík[2]

Received: 4 February 2023 / Accepted: 9 July 2023

Abstract

The Guerbet reaction is a possible way for transformation of ethanol to 1-butanol (important for many kinds of industries), which consists of four steps: dehydrogenation, aldol condensation, dehydration, and hydrogenation. Due to the elimination of possible side-reactions, the selective catalysis is required to favour production of 1-butanol at temperature below 350 °C. The main aim of this work was the ethanol transformation via heterogeneous catalysis using active Mg–Al mixed oxides with copper or cobalt carried out in the microflow reactor in the reaction temperature interval 280–350 °C. The novelty lies in the statistical analysis of results from characterization of catalyst structure and surface with catalysis results providing more sophisticated perspective on the ethanol valorization. The series of Mg–Al catalysts containing copper showed an overall higher conversion of ethanol and selectivity to butanol compared to the series containing cobalt. Major difference of catalytic activity was at low reaction temperatures and at a lower copper content in the Mg–Al matrix, which is significant from the point of view of environmentally clean processes. A multi-step mechanism of the Guerbet reaction involving an aldol condensation was verified for both tested catalysts series and reaction conditions.

Graphic abstract

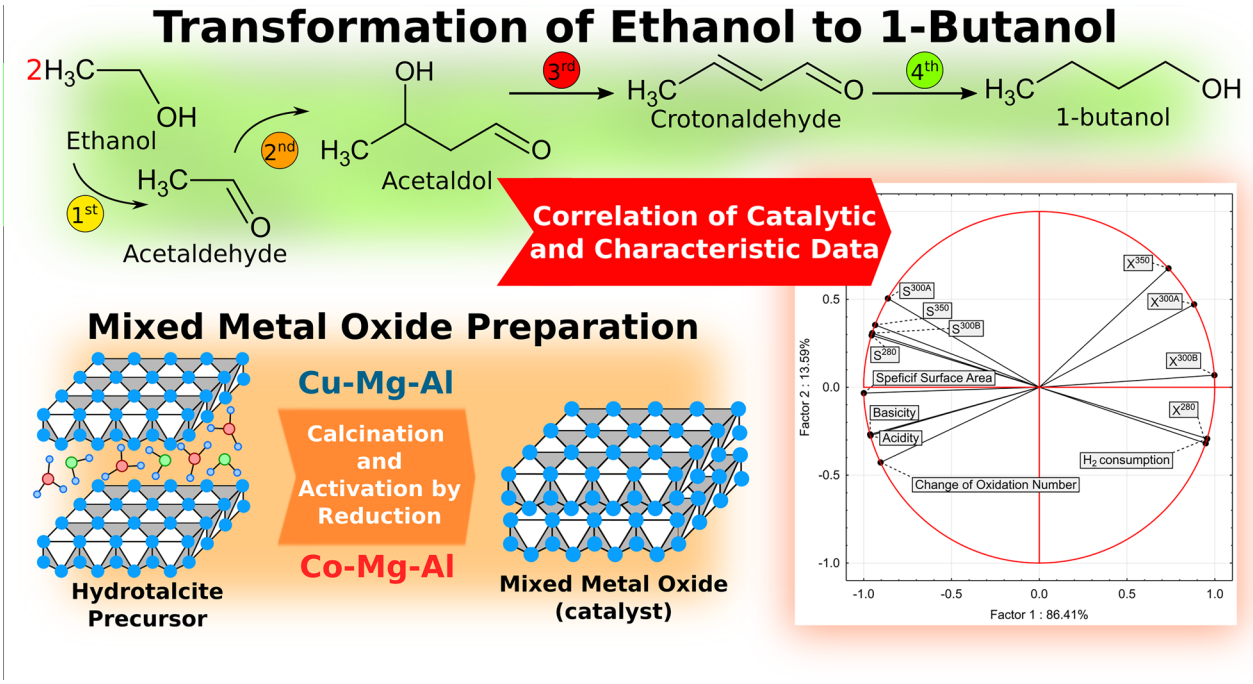

Valorization of bio-ethanol to 1-butanol by Mg-Al mixed metal oxides enhanced by Cu or Co

Keywords Guerbet reaction · Mixed metal oxide · Hydrotalcite · Copper · Cobalt

Extended author information available on the last page of the article

Published online: 29 July 2023

Abbreviations

PCA	Principal component analysis
CO_2-TPD	Temperature programmed desorption of CO_2
HT	Hydrotalcite
H_2-TPR	Temperature programmed reduction by H_2
ICP-OES	Inductively couple plasma optical emission spectrometry
MO	Mixed metal oxide
NFDLT	Nonlocal density functional theory
NH_3-TPD	Temperature programmed desorption of NH_3
XRD	X-ray diffraction analysis
S^{280}	1-Butanol selectivity at 280 °C, %
S^{300A}	1-Butanol selectivity at first 300 °C (at start of catalytic test), %
S^{300B}	1-Butanol selectivity at first 300 °C (at the end of catalytic test), %
S^{350}	1-Butanol selectivity at first 350 °C, %
X^{280}	Ethanol conversion at 280 °C, %
X^{300A}	Ethanol conversion at first 300 °C (at start of catalytic test), %
X^{300B}	Ethanol conversion at first 300 °C (at the end of catalytic test), %
X^{300B}	Ethanol conversion at first 300 °C (at the end of catalytic test), %
X^{350}	Ethanol conversion at first 350 °C,

Introduction

Ethanol, as a renewable raw material, is important source for preparation of higher alcohol and other add-value chemicals, which are currently produced from raw fossil materials. It has several conventional uses as (i) solvent, (ii) fuel for combustion engines as admixture (Somma et al. 2010) and in food industry. It can be also used for production of compounds currently produced from crude oil such as 1-butanol, 1,3-butadiene, isobutylene, acetic acid, and ethyl acetate. (Angelici et al. 2013). The studding of ethanol as a renewable alternative source is important because it is one of the possible paths to replace the crude oil (León et al. 2011), which is one of the main motivations of this work. Therefore, the valorization of ethanol to 1-butanol via heterogeneous catalysis by Mg–Al metal mixed oxides doped by transition metal (Cu or Co) was set as main goal, which included obtaining catalytic data (ethanol conversion and selectivity to 1-butanol), data from metal mixed oxides characterization and correlation of obtained data for better understanding catalytic process. 1-Butanol was chosen because of versatile use, for example, as fuel, fuel admixture, solvent (Zgheib and Takache 2021). Butanol can be also used as raw material for production of another desired products such as butyraldehyde, butyric acid, butyl acetate, and acrylate. (Mascal 2012). Last but not least, butanol can be also used as fuel or additive for internal combustion engines, improve its performance and, for example, significantly reduce the emission of NO_X (Arce-Alejandro et al. 2018). Obtaining 1-butanol from raw chemicals compounds such as ethanol is convenient competitive method to the fermentation (Al-Shorgani et al. 2012). Because ethanol can be obtained from many sources sugar, starch, etc. (Gupta and Verma 2015). But to avoid using crops grown as food, other sources can be used, such as lignino-cellulosic biomass (Mandade et al. 2016). Moreover, the producing of butanol from ethanol is in accordance with "Green deal" of EU policy (Erbach et al. 2022).

The ethanol transformations can be achieved by the so-called Guerbet reaction (Veibel and Nielsen 1967), which is a reaction of two primary alcohols to beta-alkylated secondary alcohol. The primary alcohols can be (i) two identical molecules of alcohol, such as two molecules of ethanol (called self-condensation), or (ii) two different alcohol molecules such as ethanol and 1-butanol (called cross-condensation). The Guerbet reaction consists of four consecutive steps: (i) dehydrogenation of primary alcohol, (ii) aldol, (iii) dehydration and (iv) hydrogenation (Rechi Siqueira et al. 2019) (Fig. 1). Next to the Guerbet mechanism, there are also side reactions leading to side products such as carboxylic acids, esters of these carboxylic acids and other alcohols (Mück et al. 2021). Diversion of these steps has demanding catalyst requirements and provides opportunity for heterogeneous catalysis by bi-functional catalysts (Carlini et al. 2005). Catalyst requirements include the presence of redox sites (de/hydrogenation steps), basic sites (aldol condensation step), and acidic sites (dehydration step). Higher selectivity to Guerbet alcohols, which are alcohols with two times higher molecular weight compared to starting alcohols (Hwang and Erhan 2006), can be achieved by modifying redox and acid–base properties of catalysts.

Various heterogeneous catalysts have been reported overall, for example, hydroxyapatites (Lovón-Quintana et al. 2017). Another example are bi-functional zeolites (Kots et al. 2019). But the most significant was MgO and wide group of mixed metal oxides (MO) derived from MgO, by exchanging atoms of Mg in MgO with divalent or trivalent metals (Birky et al. 2013). Wide range of materials derived from MgO was reported, for example, Mg-Fe (Cavani and Trifiro 1991). Another example could be MO of Mg–Ca (Ma et al. 2017). But the most significant MO for this work was the Mg–Al metal mixed oxide (Kikhtyanin et al. 2017). On the other hand, comparison with the other studies is difficult, due to the wide variety of reaction setups, which differ mainly in reaction temperature or in a sequence of reaction temperatures. The MO are mostly based on hydrotalcite like materials (HT) precursors, more specifically on Mg–Al layered double hydroxide (Volli and Purkait 2016). Structure of Mg–Al MO allows another tuning by transition metals.

Pure Mg–Al MOs are considered as acido–basic (Kocík et al. 2021) catalysts, but the (de)hydrogenation, acido–basic properties can be tuned by adding doping with transition metals (Huang et al. 2015). From group of heterogeneous catalysts, the Cu–Mg–Al MOs showed promising results for catalysis of Guerbet reaction, because Cu–Mg–Al dispose of bi-functional properties (Cheng et al. 2018). Despite Co–Mg–Al MOs have been studied less than Cu–Mg–Al MOs, they also provide redox properties to acid–base Mg–Al MO, i.e. Co–Mg–Al can be also classified as bi-functional catalyst as Cu–Mg–Al. Also, Co–Mg–Al MO reported higher 1-butanol selectivity compared to Mg–Al MO for Guerbet reaction (Quesada et al. 2018).

This work is focused on the transformation of ethanol to 1-butanol in the gas phase under solid catalysts and in a flow reactor. Mg–Al MO was chosen as main material because of convenient acid–base properties (Kuljiraseth et al. 2019). The modification of Mg–Al MO by transition metal was based on the previous study, which was mainly focused on the modification of Mg–Al MO by various transition metals and its influence on the Guerbet reaction (Mück et al. 2021). Moreover, the doping of Mg–Al MO by copper or cobalt was based on high alcohol dehydrogenation activity (Wu et al. 2017). The metals Cu and Co were convenient candidates to enhance Mg–Al MO. It was possible to prepare bi-functional heterogeneous catalysts, which were filling needs for the Guerbet reaction. The concentration series of Cu–Mg–Al and Co–Mg–Al were synthetised by the co-precipitation method from nitrates of respective metals; solution of sodium hydroxide was used as co-precipitating agent. Obtained HT were calcinated to MO, which were activated by reduction in stream of hydrogen at higher temperatures. Obtained MO were used to study effect of different copper or cobalt load on (i) MOs properties, (ii) ethanol conversion and (iii) 1-butanol selectivity. MOs were also deeply characterized by several experimental methods such as X-ray diffraction (XRD), inductively coupled plasma optical emission spectrometry (ICP-OES), N_2 adsorption, temperature programmed methods being temperature programmed reduction (H_2-TPR) and temperature programmed desorption of CO_2 (CO_2-TPD) or NH_3 (NH_3-TPD). Data from these characteristics were correlated with data from the catalysis such as ethanol conversion and selectivity to 1-butanol.

The main objective was achieving the highest possible ethanol conversion combined with the highest possible 1-butanol selectivity. The novelty consists of several factors: (i) comprehensive approach to the catalysis of Guerbet reaction, due to the wide variety of reaction temperatures and long term test, (ii) focus on two series of Mg–Al mixed oxide catalysts with the dopants copper or cobalt with variable content in the structure, and (iii) statistical analysis of outcomes, which enable a more comprehensive view of the reaction conditions, due to the easier detection of synergies between variables (ethanol selectivity and 1-butanol selectivity, properties of catalysts). The relation between variables would help to find catalyst with properties suitable for maximizing the ethanol conversion and butanol selectivity. Therefore, finding catalysts with convenient properties should open the path for production of 1-butanol from reliable, renewable sources.

Methods

Several methods were used in this work, such as coprecipitation (catalysts preparation), heterogeneous catalysis (catalytic tests), characterization of metal mixed oxides (catalysts) (analytical methods) and statistical analysis of catalytic data (ethanol conversion and selectivity to 1-butanol) with structural and surface properties of studied copper and cobalt mixed Mg–Al oxides.

Catalysts preparation

Two series of Mg–Al hydrotalcites with different transition metals were synthetized by co-precipitation of metal nitrates: (i) Cu–Mg–Al and (ii) Co–Mg–Al. The molar ratio of Mg:Al was kept constant at 2:1 and molar ratio of Cu (resp. Co):Al in the range from 0.05 to 0.75. This method was chosen based on previous studies where it was proven to be a reliable method capable of providing materials with a high reproducibility (Mališová et al. 2022).

The synthesis of layered double hydroxides was carried out in a double jacked batch reactor equipped with a paddle stirrer (360 rpm) at 60 °C. The amount of 250 ml of pure re-distilled was poured into reactor. The solution of metals was prepared from metal nitrates, with 1 mol dm^{-3} total concentration of metal ions: (i) $CuNO_3$, $MgNO_3$, $Al_2(NO_3)_3$ for Cu–Mg–Al and (ii) $CoNO_3$, $MgNO_3$, $Al_2(NO_3)_3$ for Co–Mg–Al. Prepared metal solution was added by peristaltic pump in to double jacked batch reactor, with flow rate 10 ml min^{-1} under stirring. The solution of NaOH (2 mol dm^{-3}) was simultaneously to maintain pH 9.5. After dosing of the entire volume of metallic solution, precipitate aged for one hour. Then, precipitate was filtrated from mother solution and flushed with re-distilled water till neutral pH of washing re-distilled water was achieved to flush residual sodium ions.

Obtained layered double hydroxides were placed into ceramic cylinders for calcination, which was carried in muffle oven with electric heating. Calcination proceeded as follows: (i) heating from laboratory temperature to 450 °C with heating rate 5 °C min^{-1}, (ii) keeping temperature of 450 °C for 4 h, and (iii) cooling to the laboratory temperature. Calcinated MO were activated by reduction of transition metals in stream of hydrogen gas (10 dm^3 h^{-1}) at 450 °C for 3 h.

Activated metal mixed oxides were transferred into glass containers, sealed, and placed to desiccator ready to be used for characterization and catalytic tests.

Catalytic tests

The catalytic tests were carried out in a flow reactor (Multi-reactor catalyst testing unit, Vinci Technologies). The mass of 2 g of catalyst was activated before reaction in the stream of hydrogen gas with flow 10 dm^3 h^{-1} and temperature at 450 °C. Flow of ethanol was set to 9 g h^{-1} and pressure in the flow reactor was set to 10 MPa. The temperature 300 °C (denoted as "300A") was kept for 32 h, then was increase to 350 °C (rate 30 °C h^{-1}) and kept for 32 h. This was followed by cooling to 280 °C (cooling rate 30 °C h^{-1}) and kept for 32 h. Finally, the temperature was raised to 300 °C with the same heating rate and kept at this value for 32 h (denoted as "300B").

Analytical methods

The real molar ratios of metals in HTs were determined by ICP-OES, 7900 ICP-OES (Agilent Technologies, USA).

The crystallographic phase composition was studied by XRD for calcinated forms of MOs. Analysis was performed on D8 Advanced diffractometer (Bruker AXS GmbH, USA), which is equipped by Cu K_α secondary graphite monochromator. Step size was 2°, and data were collected in the range 1–90°.

The N_2 adsorption isotherms were measured involving ASAP 2020 equipment (Micromeritics, USA) at temperature of liquid nitrogen (77 K) for calcinated forms of MOs. The specific surface area was calculated by the BET method. The pore diameter, volume and distribution were calculated by NFDLT method from obtained isotherms. Other details were mentioned in previous study, for example, degasification conditions (Frolich et al. 2022).

The reducibility of transition metal (Cu or Co) in MOs was determined by H_2-TPR. The basicity and acidity of MOs were determined by CO_2 and NH_3-TPD, resp. Entire TP measurements were carried out in Autochem II 2920 equipped with a TCD detector (reduction experiments), and OmniStar™ GSD 320 (Pfeiffer Vacuum, Germany) mass spectrometer (desorption experiments). Around of 100 mg of activated MO was used for each measurement. For measurements, oxygen (99.5%), helium (99.9999%), hydrogen (99.9999%), carbon dioxide (99.9999%) and ammonia (99.9999%) were used. The typical experiment consisted of pre-treatment at the calcination temperature, flushing with inert gas, cooling to RT, and saturation (TPD). The TP experiments were collected with a temperature ramp (10 °C min^{-1}) and gas flow (25 ml min^{-1}). (Smoláková et al. 2017).

The analytical methods mentioned above are described in more detail in the following previous study (Hájek et al. 2018a).

Statistical analysis

The principal component analysis (PCA) was used for correlations among the variables (Statistica 12). The PCA can be described as follows: (i) positive correlation—variables are close to each other, (ii) negative correlation variables are on the opposite sides, (iii) no correlation—angle between variables is at 90°, and (iv) distance from the centre of the circle determines how much variable contributes to individual main components (its significance) (Hájek et al. 2018a, b).

Results and discussion

Two large sets of data (catalytic and characterization of metal mixed metal oxides) were obtained and used for correlation to better understand the heterogeneous catalysis of the Guerbet reaction. The correlation data obtained were interpreted and discussed with data from other studies.

Chemical composition

The real molar ratios of metals in HT, which were used for nomenclature of HTs and MOs, are summarized in Table 1. The real contents of metals were close to the theoretical ones. Therefore, it could be considered that a preparation method with high reproducibility was chosen. The one only exception was found for HT $Co_{0.90}Mg_2Al_{1.16}$, exhibiting relatively higher content of Co and Al, which was probably

Table 1 Real molar ratios of metals in HTs (X = Cu/Co)

X-transition metal	Cu series		Co series	
Theoretical molar ratio X:Mg:Al	Real molar ratio Cu:Mg:Al	Nomenclature	Real molar ratio Co:Mg:Al	Nomenclature
0.05:2:1	0.05:2:1.06	$Cu_{0.05}Mg_2Al_{1.06}$	0.05:2:1.05	$Co_{0.05}Mg_2Al_{1.05}$
0.10:2:1	0.09:2:1.06	$Cu_{0.09}Mg_2Al_{1.06}$	0.11:2:1.06	$Co_{0.11}Mg_2Al_{1.06}$
0.25:2:1	0.23:2:1.06	$Cu_{0.23}Mg_2Al_{1.06}$	0.28:2:1.04	$Co_{0.28}Mg_2Al_{1.04}$
0.75:2:1	0.73:2:1.07	$Cu_{0.73}Mg_2Al_{1.07}$	0.90:2:1.16	$Co_{0.90}Mg_2Al_{1.17}$

caused by the pH fluctuation at the beginning of the HT synthesis (slow homogenization of reaction mixture at the beginning of coprecipitation).

Structural analysis

The successful synthesis of HTs and calcinated forms MOs was confirmed by X-ray diffraction. The diffraction lines $2\theta \approx 10.1°, 20.8°, 34.9°, 30.9°, 45.6°, 61.0°$ were attributed to hydrotalcite structure (Fig. 1) (F. Cavani et al. 1991). The diffraction lines at 20.8°, 34.9°, 30.9°, 45.6°, and 61.0° show influence of added Cu or Co. The intensity and sharpness of hydrotalcite diffraction lines were decreasing with increasing amount of Cu or Co in HTs.

After calcination of HTs, the diffraction lines at $2\theta \approx 43.0°$, 62.4° were attributed to magnesium oxides, which confirm to decomposition of layered hydrotalcite structure and formation of mixed oxides (Fig. 1) (Zhou et al. 2014). These diffraction lines were very well observed for materials with lower content of transition metals, particularly in $Cu_{0.05}Mg_2Al_{1.06}$, $Cu_{0.09}Mg_2Al_{1.06}$ and $Co_{0.05}Mg_2Al_{1.05}$, $Co_{0.11}Mg_2Al_{1.06}$. The intensity and sharpness of diffraction lines of MgO decreased with increasing content of transition metals. With increasing content of transition metal, the diffraction lines of additional oxide phases also appeared. Diffraction lines of Cu_4O_3, Cu_2MgO_3 and $MgAl_2O_4$ ($2\theta \approx 44.5°$ and 65.1°) were observed for Cu–Mg–Al series. The presence of these metal oxides was not observed in previous studies except $MgAl_2O_4$ which was also observed in case of cobalt series (Rechi Siqueira et al. 2019). The additional oxides were also observed in cobalt series, such as Co_3O_4 (Lv et al. 2013). Another observed oxide was the $CoAl_2O_4$ with major contribution at $2\theta \approx 36.8°$ (Zawadzki et al. 2011).

Surface analysis

The adsorption isotherms of N_2 at 77 K were obtained for reduced (activated) forms of MOs (Fig. 2). All isotherms are of type IV, which is typical for mesoporous materials with capillary condensation (Muttakin et al. 2018). The hysteresis loops were present for each MO, type of these hysteresis loops was between H2 and H3, which pointed out to wide distribution of pore shape. H2 is mostly related to the complex porous structure (with a pore blocking), and H3 is associated with plate-like particles or aggregates with slit-shape pores (Thommes et al. 2015).

Minor changes were observed for adsorption isotherms with increasing amount of copper or cobalt in MOs (Fig. 2 A Cu–Mg–Al series, B Co–Mg–Al series). These changes were observed only in hysteresis region (relative pressure from 0.4 to 1.0) and can be described as shift between H2 and H3 hysteresis loop and growth of plateau at the end of hysteresis loop (relative pressure range from 0.9 to 1.0). Thus, $Cu_{0.05}Mg_2Al_{1.06}$ and $Co_{0.05}Mg_2Al_{1.05}$ had wide H2 hysteresis loop. $Cu_{0.23}Mg_2Al_{1.06}$ and $Co_{0.28}Mg_2Al_{1.04}$ had hysteresis loop between H2 and H3. This shift was also accompanied by shrinking of the area between adsorption

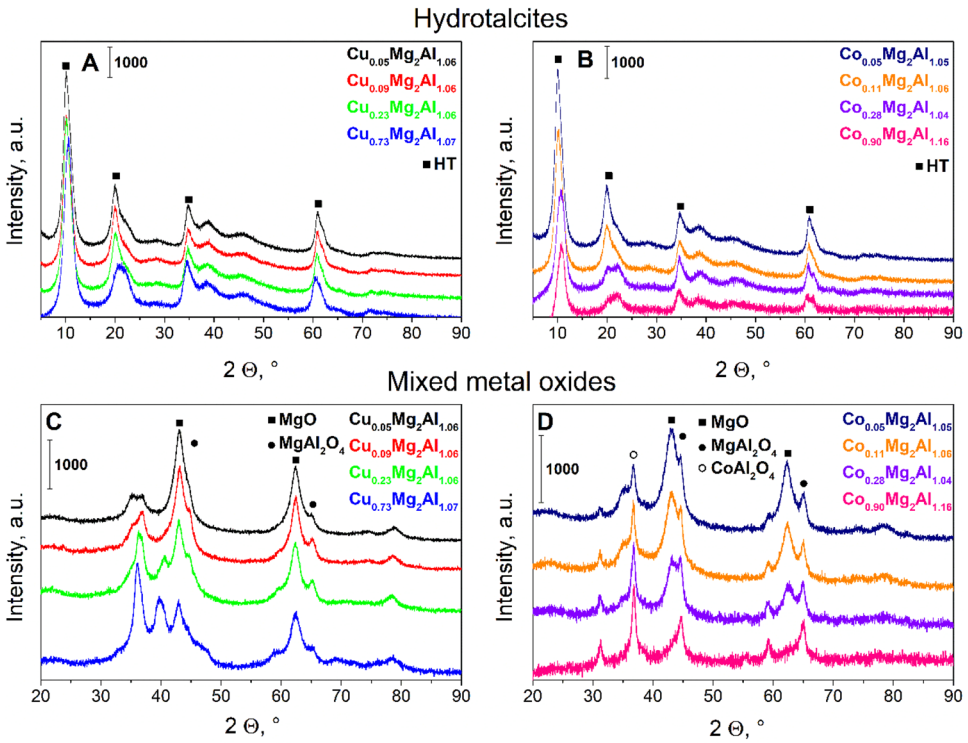

Fig. 1 XRD diffraction lines of HTs: Cu–Mg–Al **A** and Co–Mg–Al **B** calcinated MOs: Cu–Mg–Al **C** and Co–Mg–Al **D**

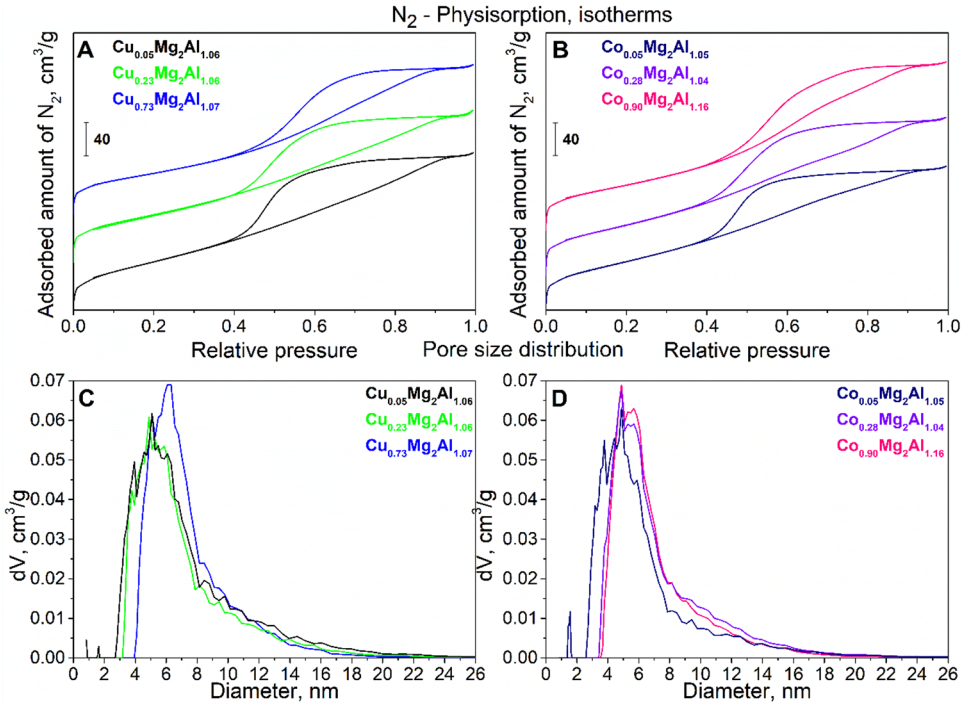

Fig. 2 Adsorption isotherms of reduced MOs: Cu–Mg–Al **A** and Co–Mg–Al **B** pore distribution of reduced MOs: Cu–Mg–Al **C** and Co–Mg–Al **D**

and desorption isotherms with increasing amount of copper in MOs. Shift to H3 hysteresis loop was completed with $Cu_{0.73}Mg_2Al_{1.07}$ and $Co_{0.90}Mg_2Al_{1.16}$.

Hysteresis loop shift was also very well recognized at pore size distribution (Fig. 2 C Cu–Mg–Al series, D Co–Mg–Al series). All Cu–Mg–Al MOs had pore size distribution located in mesoporous range (from 2 to 50 nm); only $Cu_{0.05}Mg_2Al_{1.06}$ had small contribution of micropores. Pore size distribution had similar profile for all MOs series Cu–Mg–Al, only maxima were shifted according to amount of copper in MOs. Thus, $Cu_{0.73}Mg_2Al_{1.07}$ had maximum of pore size distribution shifted to higher diameter, which was 6.1 nm. Despite these differences, $Cu_{0.05}Mg_2Al_{1.06}$ and $Cu_{0.23}Mg_2Al_{1.06}$ had the closest shape of adsorption isotherms, which is also very well recognized at pore size distribution.

Both MOs series had similar changes, respectively, to amount of transition metal in MOs. But differences were observed by close comparison of the series. Cu–Mg–Al series had larger area of hysteresis loop and larger plateau at the end of hysteresis loop (relative pressure from 0.9 to 1.0) compared to Co–Mg–Al series. This phenomenon was also observed in case of pore size distribution. Co–Mg–Al MOs had narrower pore size distribution compared to Cu–Mg–Al MOs. It can be stated, MOs with wide molar ratios of copper or cobalt were prepared, but structural properties were quite similar for these MOs.

The specific surface areas and pore volumes are summarized in Table 2. For Cu–Mg–Al MOs, the decreasing trend of specific surface area was observed with increasing amount of copper in MOs. Thus, the specific surface area ranged from 192 $m^2\ g^{-1}$ ($Cu_{0.73}Mg_2Al_{1.07}$) to 257 $m^2\ g^{-1}$ ($Cu_{0.05}Mg_2Al_{1.06}$). On the other hand, for Co–Mg–Al MOs, no relation of specific surface area with amount of cobalt was observed.

Table 2 N_2-physisorption of reduced MOs: surface area

Cu series	$m^2\ g^{-1}$	Co series	$m^2\ g^{-1}$
$Cu_{0.05}Mg_2Al_{1.06}$	257	$Co_{0.05}Mg_2Al_{1.05}$	221
$Cu_{0.23}Mg_2Al_{1.06}$	218	$Co_{0.28}Mg_2Al_{1.04}$	251
$Cu_{0.73}Mg_2Al_{1.07}$	192	$Co_{0.90}Mg_2Al_{1.16}$	221

Reducibility of copper and cobalt

Reduced (activated) MOs Cu–Mg–Al and Co–Mg–Al were re-oxidized before H_2-TPR and after that standard H_2 reduction curves were obtained (Fig. 3 A Cu–Mg–Al series, B Co–Mg–Al series). For Cu–Mg–Al series, the reduction proceeded in one temperature interval (60–405 °C). On the contrary, for Co–Mg–Al, the reduction proceeded in two separated temperature intervals (70–705 °C and 700–1100 °C).

Systematic changes related to the amount of transition metal were observed in both series, such as peak intensity, area, shape, and peak position (Fig. 3). Peak intensity and area under peak were increasing with increasing amount of copper for Cu–Mg–Al series or with increasing amount of cobalt for Co–Mg–Al series. Maxima of reduction peak was shifting towards the lower temperatures with

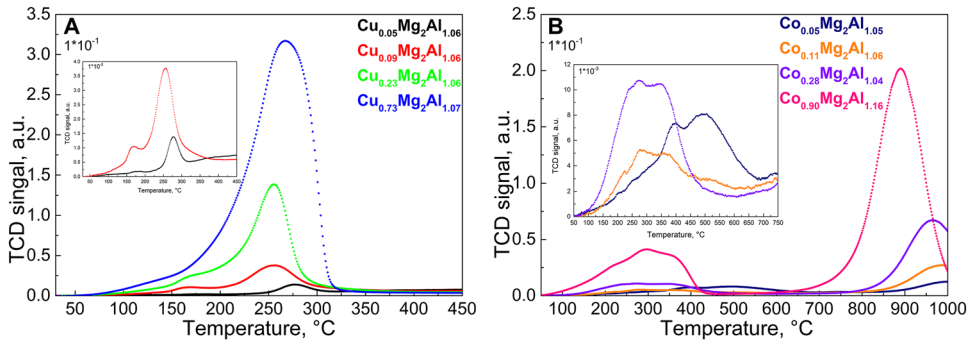

Fig. 3 H_2-TPR for reduced MOs Cu–Mg–Al **A** and Co-Mg–Al **B**

Table 3 Average change of oxidation state of transition metals in MOs

Cu series		Co series	
$Cu_{0.05}Mg_2Al_{1.06}$	1.7	$Co_{0.05}Mg_2Al_{1.05}$	1.7
$Cu_{0.09}Mg_2Al_{1.06}$	1.5	$Co_{0.11}Mg_2Al_{1.06}$	0.4
$Cu_{0.23}Mg_2Al_{1.06}$	1.0	$Co_{0.28}Mg_2Al_{1.04}$	0.4
$Cu_{0.73}Mg_2Al_{1.07}$	1.0	$Co_{0.90}Mg_2Al_{1.16}$	1.0

increasing amounts of transition metal in all MOs. For Cu–Mg–Al series was shift of the maxima in range from 257 to 278 °C and for Co–Mg–Al series was shift of the maxima observed between 300 and 500 °C. Similarly, reduction temperature interval was expanding with increasing amount of copper, and expansion of reduction temperature was observed from 225 to 325 °C ($Cu_{0.05}Mg_2Al_{1.06}$) to 70–375 °C ($Cu_{0.73}Mg_2Al_{1.07}$). On the other hand, amount of cobalt had opposite influence, and therefore, increasing amount of cobalt led to narrowing of reduction temperature interval, i.e. reduction of cobalt was in temperature intervals from 70–457 °C ($Co_{0.90}Mg_2Al_{1.16}$) to 70–705 °C ($Co_{0.05}Mg_2Al_{1.05}$). This shifting can be caused by changing interactions of copper or cobalt with Mg–Al matrix (Jiang et al. 2005).

Systematic changes were related to the amount of copper in Cu–Mg–Al series, such as peak intensity, area, shape, and peak position (Fig. 3 A Cu-Mg–Al series). Peak intensity and area under peak were increasing with increasing amount of copper in MOs from Cu–Mg–Al series.

Change of oxidation number of transition metals in MOs were calculated from the consumptions of H_2 (area under the reduction curve) related to the total amount of the metal in the oxide and taking to account a simple reduction of CuO or CoO to metals in the MOs. Previous results showed that only transition metal oxides are reduced in the temperature interval (Benito et al. 2019). Results are summarized in

Table 3. Decreasing trend was observed for dependency of change of oxidation number on copper content in Cu–Mg–Al series. Co–Mg–Al series had no specific trend, i.e. significant decrease of change of oxidation number was observed between $Co_{0.05}Mg_2Al_{1.05}$ and $Co_{0.11}Mg_2Al_{1.06}$, followed by increase between $Co_{0.28}Mg_2Al_{1.04}$ and $Co_{0.90}Mg_2Al_{1.16}$. Low theoretical change of oxidation number can be caused by several factors. It can be caused by inaccessibility of all amounts of copper or cobalt for reduction. Another factor can be presence of non-stoichiometric transition metal oxides, which could stabilize copper or cobalt. Also, not all amount of copper or cobalt may have been re-oxidized to oxidation state + 2 during pre-treatment, due to better stability. In case of cobalt, determination of theoretical change of oxidation number is more complicated, because of the presence of reduction peak at high temperatures above 700 °C. It can be another evidence of Co_3O_4 or $CuAl_2O_4$ presence (Pérez et al. 2014), which was already proven by XRD analysis.

Acid–base properties

Basic and acidic properties were described by the desorption of CO_2 and NH_3 probes. Results of TPD experiments are summarized in Fig. 4 for all reduced MOs (Basic properties: Cu–Mg–Al (A), Co–Mg–Al (B); Acidic properties: Cu–Mg–Al series (C), Co–Mg–Al (D)).

The amount of basic sites was dependent on the composition of Cu–Mg–Al MOs. With increasing copper content in Cu–Mg–Al series the amounts of basic sites were decreasing (Table 4). These amounts of basic sites ranged from 223 µmol CO_2 g^{-1} for $Cu_{0.05}Mg_2Al_{1.06}$ to 155 µmol CO_2 g^{-1} for $Cu_{0.73}Mg_2Al_{1.07}$. On the other hand, amount of basic sites was not that dependent on the composition of Co–Mg–Al MOs. Co–Mg–Al series had narrow distribution of amounts of basic sites. It ranged from 220 µmol CO_2 g^{-1} to 191 µmol CO_2 g^{-1} (Table 4). $Co_{0.05}Mg_2Al_{1.05}$ and $Co_{0.11}Mg_2Al_{1.06}$ and $Co_{0.28}Mg_2Al_{1.04}$ exhibited almost the same amounts of basic sites around 220 µmol CO_2 g^{-1}. For all materials of Cu–Mg–Al and Co–Mg–Al series, CO_2-TPD record maxima were located around temperature 110 °C and range of these curves is from 40 °C to 450 °C. CO_2-TPD records were related to overlapped peaks (Fig. 4) pointing to the presence of weak, medium-strong and strong basic sites on the catalysts surface (Smoláková et al. 2017). Profiles of

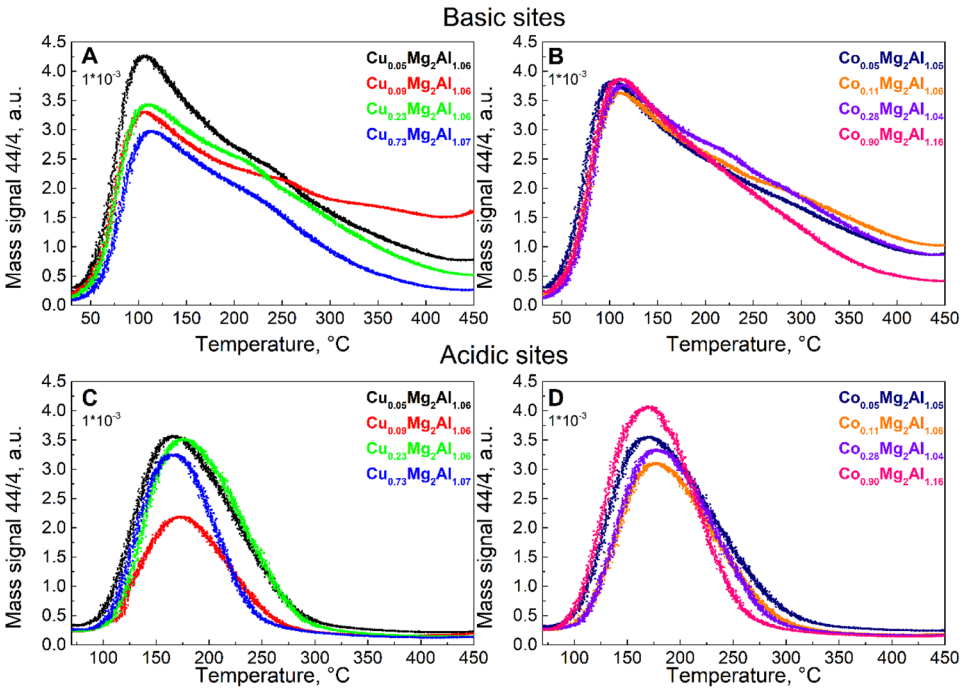

Fig. 4 Basic: Cu–Mg–Al **A**, Co–Mg–Al **B**; acidity: Cu–M–Al **C**, Co–Mg–Al **D**

Table 4 Amounts of basic and acidic sites for reduced MOs

Cu series	Basicity, μmol g^{-1}	Acidity, μmol g^{-1}	Co series	Basicity, μmol g^{-1}	Acidity, μmol g^{-1}
$Cu_{0.05}Mg_2Al_{1.06}$	223	223	$Co_{0.05}Mg_2Al_{1.05}$	220	250
$Cu_{0.09}Mg_2Al_{1.06}$	212	68	$Co_{0.11}Mg_2Al_{1.06}$	219	104
$Cu_{0.23}Mg_2Al_{1.06}$	155	114	$Co_{0.28}Mg_2Al_{1.04}$	218	109
$Cu_{0.73}Mg_2Al_{1.07}$	140	91	$Co_{0.90}Mg_2Al_{1.16}$	191	128

these overlapped peaks were not dependent on the catalyst composition, i.e. amount of copper or cobalt had no influence on peaks profile (Fig. 4). It can be concluded that distribution of weak, medium-strong and strong basic sites was the similar for all MOs in the Cu–Mg–Al and Co–Mg–Al series. This distribution is rough, because determination of the basic centres strength based only on CO_2 temperature programmed desorption was not possible. On the other hand, strength of the basic sites is related to the desorption temperature of CO_2, i.e. the desorption temperature of CO_2 was able to provide initial information about the basic centres distribution (Pavel et al. 2012).

Amounts of acidic sites ranged from 68 μmol NH_3 g^{-1} to 223 μmol NH_3 g^{-1} for Cu–Mg–Al series and from 128 μmol NH_3 g^{-1} to 250 μmol NH_3 g^{-1} for Co–Mg–Al series (Table 4). Single desorption peak was observed in temperature range from 80 °C to 300 °C with maxima around 175 °C (Fig. 4), without any sign of merging peaks, for all materials of Cu–Mg–Al and Co–Mg–Al series. Therefore, the only one type of acidic sites was suggested. On the other hand, temperature range was changing slightly, which could be caused by stronger interactions of ammonia and transition metal in MOs or by diffusion in porous structure of MOs (Dixit et al. 2013).

Co–Mg–Al series reached over all higher amounts of basic and acidic sites compared to Cu–Mg–Al series. Co–Mg–Al series had also more uniform CO_2 and NH_3 desorption curves compared to Cu–Mg–Al series. It is therefore possible to assume that Co–Mg–Al series bear higher amounts of basic and acidic sites compared to Cu–Mg–Al series.

Ethanol transformation

The results of catalysis (ethanol conversion (X) and selectivity (S) to 1-butanol) at tree reaction temperatures for reduced forms of Cu–Mg–Al and Co–Mg–Al oxides are summarized in Fig. 5. These experiments follow up previous study focused on the Guerbet reaction catalysed by Mg–Al MO and Mg–Al MO doped by several transition metals (Cu, Co, Mn, Cr) (Mück et al. 2021).

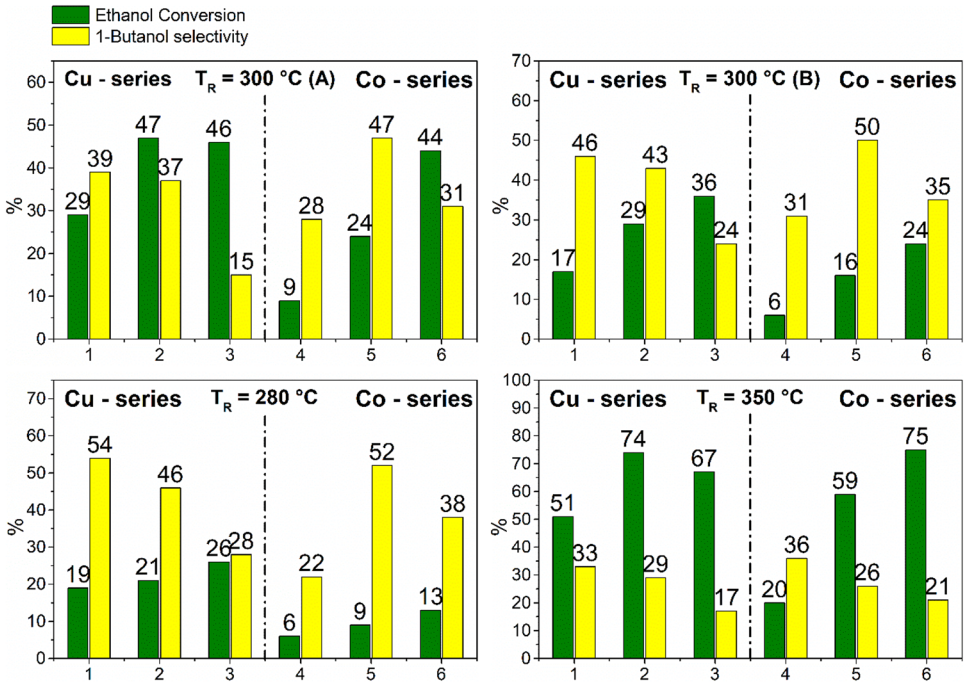

Fig. 5 Ethanol conversion and 1-butanol selectivity (1—Cu0.05Mg2Al1.06, 2—Cu0.23Mg2Al1.06, 3—Cu0.73Mg2Al1.07, 4—Co0.05Mg2Al1.05, 5—Co0.28Mg2Al1.04, 6—Co0.90Mg2Al1.16)

The ethanol conversion follows the course of reaction temperature during the experiment, but change of the ethanol conversion was observed in each reaction temperature section (Figure S1). The course of reaction temperature was set as follows: (i) start at 300 °C (300A), (ii) heating to 350 °C, (iii) cooling to 280 °C, and (iv) heating to 300 °C (300B). Each temperature was held for 32 h. Samples of liquid and gas phase were taken every 4 h during the time of 32 h for each temperature. Therefore, the number of 8 samples were taken for each reaction temperature. Catalytic data (ethanol conversion and 1-butanol selectivity) were obtained, and average value of these data were presented, as it is displayed in Figure S1.

Decrease of the ethanol conversion was observed during first 32 h for every catalyst at the reaction temperature 300 °C (300A), greater decrease of the ethanol conversion from was observed for catalysts from cobalt series. The increase in reaction temperature to 350 °C led to the increase in ethanol conversion. Minor changes in ethanol conversion were observed during this reaction temperature compared to the catalysts activity at 300 °C (300A). Therefore, catalytic activity was close to the equilibrium. The change of the reaction temperature to 280 °C caused huge drop of the ethanol conversion, but there were no further changes of catalytic activity at this reaction temperature for all catalysts, i.e. catalysts were stable by the time of reaching 280 °C. The last reaction temperature was set back to 300 °C (300B) to verify catalysts stability, which lead to the increase in catalytic activity compared to the previous catalyst activity at 280 °C. The ethanol conversion remained constant at this temperature. Therefore, long-term catalytic tests proved catalysts from both series to be active and stable by the time reaching 66 h in reaction, which was confirmed by rise of reaction temperature from 280 °C to 300 °C. Stable course (minor increase) of the ethanol conversion during time at the reaction temperature 300 °C (300B).

The ethanol conversion was in large range (Fig. 5) and generally increased with two factors: (i) increasing reaction temperature and (ii) increasing copper content in Cu–Mg–Al MOs or cobalt content in Co–Mg–Al MOs. The reaction temperature had great impact on the ethanol conversion, as it was observed for the reaction temperature of 280 °C and 350 °C. The greatest increase in ethanol conversion was recorded for the $Cu_{0.23}Mg_2Al_{1.06}$ catalyst, where conversion increased from 21% at 280 °C to 74% at 350 °C. On the other hand, the influence of the transition metal is more complicated due to more factors involved (acido–basic properties, specific surface area, phases of oxides, etc.). Overall, it is possible to consider the positive influence of transition metal in Mg–Al MO on the ethanol conversion, i.e., ethanol conversion increased with increasing copper or cobalt content in Cu/Co–Mg–Al MO. On closer comparison, the ethanol conversion did not increase further when comparing $Cu_{0.23}Mg_2Al_{1.06}$ and $Cu_{0.73}Mg_2Al_{1.07}$, despite similar redox properties, demonstrated by the average change of oxidation state of copper these two catalysts. Decreasing specific surface area with increasing amount of copper could be linked to the ethanol conversion when comparing $Cu_{0.23}Mg_2Al_{1.06}$ and $Cu_{0.73}Mg_2Al_{1.07}$. In addition, higher copper content may be related to the particle agglomeration, and however, these

data are not available in this study. Therefore, it was possible to state, that optimal composition of Cu–Mg–Al MO for catalysis of the Guerbet reaction lied between the two compositions $Cu_{0.23}Mg_2Al_{1.06}$ and $Cu_{0.73}Mg_2Al_{1.07}$. Co–Mg–Al catalysts did not reveal such behaviour; the ethanol conversion was increasing with the increasing cobalt content in Co–Mg–Al MO in a whole studied range. On the other hand, the catalyst from cobalt series was less active at lower temperatures and at lower amounts of transition metal compared to the copper series.

The selectivity of 1-butanol decreased with increasing ethanol conversion (Fig. 5), i.e. higher ethanol conversion means lower selectivity of 1-butanol, due to higher probability of side products formation such as higher alcohols, carboxylic acids, and ethers. (Mück et al. 2021). On the other hand, selectivity of 1-butanol increased with increasing ethanol conversion for $Co_{0.05}Mg_2Al_{1.05}$, which was probably due to overall low conversions of ethanol. Acidobasic properties and specific surface area of catalysts were other factors involved in the selectivity to 1-butanol. Therefore, decreasing acidity, basicity, and specific surface lead to the decreasing 1-butanol selectivity, which was observed by comparing catalysts with similar ethanol conversion such as $Cu_{0.23}Mg_2Al_{1.06}$ and $Cu_{0.73}Mg_2Al_{1.07}$. These catalysts had similar conversion of ethanol, but differences (decreasing trend with increasing amounts of copper) between selectivity to 1-butanol, basicity, and specific surface area were high values. Similar trend was observed for catalysts $Cu_{0.05}Mg_2Al_{1.06}$, and $Cu_{0.23}Mg_2Al_{1.06}$. Therefore, it was possible to consider high importance of acidobasic properties, and specific surface area of catalysts for the Guerbet reaction. Further, all data from characterization and catalysis will be treated by PCA statistical analysis ("Statistical correlation") to reveal all potential relations.

The direct comparison of catalytic data with other studies is relatively difficult, due to (i) high variability of heterogeneous/homogeneous catalysts and (ii) wide range of reaction conditions including type of reactor. Many types of catalyst such as zeolites, hydroxyapatite, supported metal catalyst or metal mixed oxides with different metals or metal ratios were studied. The reaction conditions differed in many ways such as type of reactor batch or flow and ratio between catalyst and ethanol. The reaction temperatures were in large range from 80 °C to 400 °C, also pressure was in large range from 0.1 to 10 MPa and time of reaction from 2 h catalytic test to long-term test reaching over 150 h, which is also the case of this work. Ethanol conversion was in large range from 0 to 85%, due to the facts mentioned above (Gabriëls et al. 2015).

The data obtained from heterogeneous catalysis of the Guerbet reaction confirm that both series of MO at given conditions were competitive to findings in previous studies (Mück et al. 2021). Therefore, it is possible to state that Co–Mg–Al and especially Cu–Mg–Al metal mixed oxides have protentional for further tuning to reach even higher conversion of ethanol followed by high 1-butanol selectivity.

Statistical correlation

The results were statistically analysed by PCA to discovered of hide relation between all variables (characterization of catalyst and catalyst activity), because it is multivariable system (Fig. 6). The blue coloured variables represent the data from characterization, and black coloured variables represent the catalytic data. Therefore, it can show relations between multiple variables which does not have clear relations just by simple comparing. The statistical analysis is almost always omitted in other papers, although it can provide deeper understanding of the Guerbet reaction heterogeneous catalysis (Chieregato et al. 2015; Metzker et al. 2021; Davies et al. 2022).

Cu–Mg–Al and Co–Mg–Al series showed similar cluster of variables (Fig. 6), which was H_2 consumption with

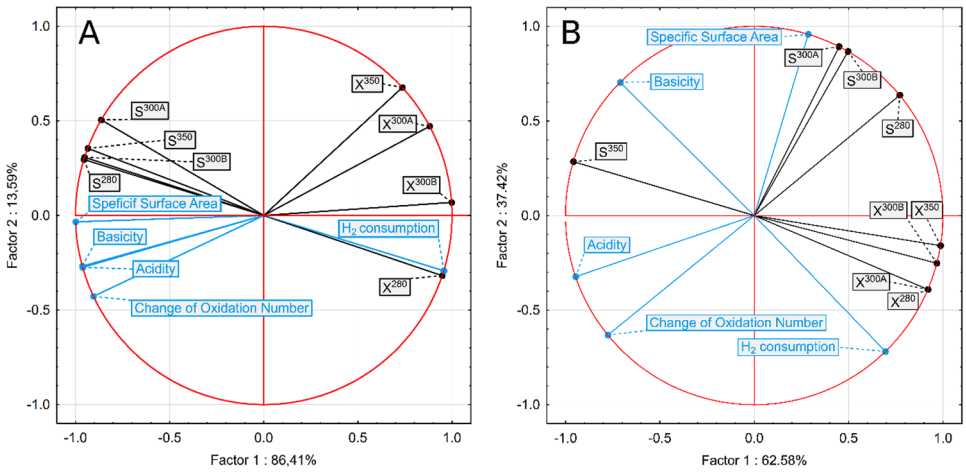

Fig. 6 Characterization and catalytic data correlation for Cu–Mg–Al **A** and Co–Mg–Al **B**

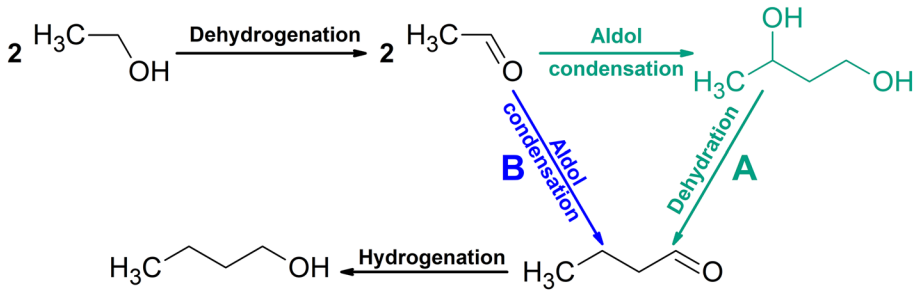

Fig. 7 **A** Four-step mechanism of the Guerbet reaction, **B** three-step mechanism

ethanol conversion (X^{280}, X^{300A}, X^{300B}, X^{350}), which was H_2 consumption with ethanol conversion (X^{280}, X^{300A}, X^{300B}, X^{350}). On the other hand, rest of variables were not similar for studied series of catalysts.

Cu–Mg–Al series showed another cluster of variables with positive correlation except H_2 consumption and ethanol conversion (X^{280}, X^{300A}, X^{300B}, X^{350}), which was cluster of basicity, acidity, specific surface area and selectivity to 1-butanol (S^{280}, S^{300A}, S^{300B}, S^{350}) (Fig. 6 A). Negative correlation between these two variables clusters of Cu-Mg–Al was observed. Therefore, redox sites (properties) and H_2 consumption were in negative correlation, for example, to the acido-basic properties and selectivities. Co–Mg–Al series showed another two clusters of variables except H_2 consumption and ethanol conversion (X^{280}, X^{300A}, X^{300B}, X^{350}): (i) second group is specific surface area and 1-butanol selectivity (S^{280}, S^{300A}, S^{300B}) and (ii) third group is acidity, basicity, and 1-butanol selectivity (S^{350}) (Fig. 6 B).

Strong positive correlation of H_2 consumption and the ethanol conversion proved the importance of the redox properties of catalysts for the Guerbet reaction, because of the first step, which is dehydrogenation of primary alcohol(s) and redox properties are needed. Therefore, copper or cobalt, as metals with great redox properties, proved to be necessary dopant in Mg–Al matrix for the reaction. On the other hand, correlation of H_2 consumption and the ethanol conversion growth weaker with increasing temperature, which was caused by stronger dependency of the Guerbets reaction first step on the reaction temperature. Therefore, if catalysts dispose of redox properties, the reaction can be carried out at lower reaction temperatures, which can provide economic and ecological benefits.

Positive correlation of the acido-basic properties and selectivity to 1-butanol proved the necessity of acido-basic centres presence, because the second step of the Guerbet reaction is aldol condensation of two molecules of aldehydes formed in the first step, which is catalysed by the basic centres (properties). Obtained hydroxyaldehyde from the second step continues to the third steps of the Guerbet reaction, which is dehydration to the unsaturated aldehyde and its catalysed by the acid centres (properties). Therefore, both centres were needed for the reaction. On the other hand, the stronger correlation of the basicity and selectivity to 1-butanol compared to the correlation of acidity and selectivity to 1-butanol was caused by order of reaction steps, as it was mentioned above. Aldol condensation proceeds the dehydration; hence, the selectivity to 1-butanol depends more on the basic centres. The acido-basic properties were not the only factor involved in the selectivity to 1-butanol because of the specific surface area, which is so-called steric selectivity. Major impact of the specific surface area was observed in case of catalysis by cobalt series. Therefore, selectivity to 1-butanol was more affected by specific surface at lower reaction temperatures (280 °C, 300 °C), but at higher reaction temperature it was more affected by acido-basic properties.

Four-step mechanism of the Guerbet reaction, which was described in more detail in previous study (Mück et al. 2021), was confirmed by correlation of catalytic and characteristic data. Therefore, mechanism of direct alcohols condensation is less probable (Xu et al. 2014). The confirmation of the four-step mechanism, which is slightly different from the three-step mechanism (Fig. 7) (Wingad et al. 2016), which consider only dehydrogenation of two primary alcohols, aldol condensation of obtained aldehydes to unsaturated aldehydes, and hydrogenation to beta-alkylated alcohol. Therefore, the three-step mechanism does not involve dehydration step of unsaturated aldehydes, which is crotonaldehyde in case of the Guerbet reaction for ethanol. Crotonaldehyde was observed during the previous studies (Chieregato et al. 2015) and at this study as the intermediate of the Guerbet reaction for ethanol.

Conclusion

The work analysed heterogeneous catalysis (Cu–Mg–Al and Co–Mg–Al metal oxides) for ethanol transformation to 1-butanol. The molar ratio of Mg:Al was kept at 2:1 and molar ratio of transition metal to alumina was in range from 0.05 to 0.73 for Cu:Al and from 0.05 to 0.90 for Co:Al. The mixed metal oxides with similar textural properties were prepared, despite wide range of concentrations of copper or

cobalt. On the other hand, change of oxidation number of transition metal, basicity and acidity were influenced by kind and concentration of transition metal in mixed metal oxide.

The ethanol conversion and selectivity of 1-butanol were determined. The positive contribution of transition metal was observed for ethanol conversion, i.e. the catalysts with larger amount of transition metal were more active. The highest value of ethanol conversion was almost the same for Cu–Mg–Al and Co–Mg–Al series. The increasing ethanol conversion caused lower 1-butanol selectivity, due to side products formation. Nevertheless, catalyst from the copper series performed better compared to the catalysts from cobalt series. They were more active at lower reaction temperatures, which is convenient from economic and ecological point of view, because copper is cheaper and less harmful to the environment. The correlations were made for outcomes from catalyst characterization and ethanol transformation and provided view on the relations between all studied variables with more, i.e. the correlations summarized and reveal the interactions between the variables took into consideration. It can be stated that these correlations may be one of the proofs of the four-step mechanism of the Guerbet reaction. It is newer point of view compared to the previous three-step mechanism, which did not include dehydration step of hydroxy aldehyde(s).

Promising results allow further development of this ethanol valorization to obtain another renewable source (ethanol) for production of more valuable chemical compounds such as 1-butanol. Therefore, whole process can be not only reliable, but also more clean and environmentally friendly and less dependent on crude oil.

Supplementary Information The online version contains supplementary material available at https://doi.org/10.1007/s10098-023-02581-5.

Acknowledgements This work was supported by the University of Pardubice, Czech Republic, project SGS_2023_008. The result was achieved using the infrastructure included in the project Efficient Use of Energy Resources Using Catalytic Processes (LM2018119) which has been financially supported by MEYS within the targeted support of large infrastructures.

Author contributions KF, JM, MH wrote the main manuscript text. JM prepared all figures. JM performed catalytic tests and also contributed to manuscript. JK was consultant. All authors reviewed the manuscript.

Funding Open access publishing supported by the National Technical Library in Prague.

Data availability Enquiries about data availability should be directed to the authors.

Declarations

Competing interests The authors declare no competing interests.

References

Al-Shorgani NKN, Kalil MS, Ali E et al (2012) The use of pretreated palm oil mill effluent for acetone–Butanol–Ethanol fermentation by *Clostridium saccharoperbutylacetonicum* N1-4. Clean Technol Environ Policy 14:879–887. https://doi.org/10.1007/s10098-012-0456-7

Angelici C, Weckhuysen BM, Bruijnincx PCA (2013) Chemocatalytic conversion of ethanol into butadiene and other bulk chemicals. Chemsuschem 6:1595–1614. https://doi.org/10.1002/cssc.201300214

Arce-Alejandro R, Villegas-Alcaraz JF, Gómez-Castro FI et al (2018) Performance of a gasoline engine powered by a mixture of ethanol and n-butanol. Clean Technol Environ Policy 20:1929–1937. https://doi.org/10.1007/s10098-018-1584-5

Benito P, Vaccari A, Antonetti C et al (2019) Tunable copper-hydrotalcite derived mixed oxides for sustainable ethanol condensation to n-butanol in liquid phase. J Clean Prod 209:1614–1623. https://doi.org/10.1016/j.jclepro.2018.11.150

Birky TW, Kozlowski JT, Davis RJ (2013) Isotopic transient analysis of the ethanol coupling reaction over magnesia. J Catal 298:130–137. https://doi.org/10.1016/j.jcat.2012.11.014

Carlini C, Marchionna M, Noviello M et al (2005) Guerbet condensation of methanol with n-propanol to isobutyl alcohol over heterogeneous bifunctional catalysts based on Mg–Al mixed oxides partially substituted by different metal components. J Mol Catal A Chem 232:13–20. https://doi.org/10.1016/j.molcata.2004.12.037

Cheng FL, Guo HQ, Cui JL et al (2018) Guerbet reaction of methanol and ethanol catalyzed by $CuMgAlO_x$ mixed oxides: effect of M^{2+}/Al^{3+} ratio. Ranliao Huaxue Xuebao/j Fuel Chem Technol 46:1472–1481. https://doi.org/10.1016/s1872-5813(18)30061-6

Chieregato A, Ochoa JV, Bandinelli C et al (2015) On the chemistry of ethanol on basic oxides: revising mechanisms and intermediates in the lebedev and Guerbet reactions. Chemsuschem 8:377–388. https://doi.org/10.1002/cssc.201402632

Davies AM, Li ZY, Stephenson CRJ, Szymczak NK (2022) Valorization of ethanol: ruthenium-catalyzed Guerbet and sequential functionalization processes. ACS Catal 12:6729–6736. https://doi.org/10.1021/acscatal.2c01570

Dixit M, Mishra M, Joshi PA, Shah DO (2013) Physico-chemical and catalytic properties of Mg–Al hydrotalcite and Mg–Al mixed oxide supported copper catalysts. J Ind Eng Chem 19:458–468. https://doi.org/10.1016/j.jiec.2012.08.028

Erbach G, Jensen L, Chahri S, Claros E (2022) Briefing towards climate neutrality. https://www.europarl.europa.eu/thinktank/en/document/EPRS_BRI(2022)733513

Cavani F, Trifiro AV (1991) Hydrotalcite-type anionic clays: preparation, properties and applications. Catal Today 11:173–301. https://doi.org/10.1007/BF03263563

Frolich K, Kocík J, Mück J et al (2022) The role of Zn in the Cu–Zn–Al mixed oxide catalyst and its effect on glycerol hydrogenolysis. Mol Catal. https://doi.org/10.1016/j.mcat.2022.112796

Gabriëls D, Hernández WY, Sels BF et al (2015) Review of catalytic systems and thermodynamics for the Guerbet condensation reaction and challenges for biomass valorization. Catal Sci Technol 5:3876–3902. https://doi.org/10.1039/c5cy00359h

Gupta A, Verma JP (2015) Sustainable bio-ethanol production from agro-residues: a review. Renew Sustain Energy Rev 41:550–567. https://doi.org/10.1016/j.rser.2014.08.032

Hájek M, Tomášová A, Kocík J, Podzemná V (2018a) Statistical evaluation of the mutual relations of properties of Mg/Fe hydrotalcites and mixed oxides as transesterification catalysts. Appl Clay Sci 154:28–35. https://doi.org/10.1016/j.clay.2017.12.039

Hájek M, Vávra A, Skopal F et al (2018b) Biodiesel: the study of methyl esters loss in the glycerol phase at various conditions. J Clean Prod 197:1573–1578. https://doi.org/10.1016/j.jclepro.2018.06.287

Huang X, Atay C, Korányi TI et al (2015) Role of Cu–Mg–Al mixed oxide catalysts in lignin depolymerization in supercritical ethanol. ACS Catal 5:7359–7370. https://doi.org/10.1021/acscatal.5b02230

Hwang HS, Erhan SZ (2006) Synthetic lubricant basestocks from epoxidized soybean oil and Guerbet alcohols. Ind Crops Prod 23:311–317. https://doi.org/10.1016/j.indcrop.2005.09.002

Jiang Z, Hao Z, Yu J et al (2005) Catalytic combustion of methane on novel catalysts derived from Cu–Mg/Al-hydrotalcites. Catal Letters 99:157–163. https://doi.org/10.1007/s10562-005-2108-6

Kikhtyanin O, Čapek L, Smoláková L et al (2017) Influence of Mg–Al mixed oxide compositions on their properties and performance in aldol condensation. Ind Eng Chem Res 56:13411–13422. https://doi.org/10.1021/acs.iecr.7b03367

Kocík J, Hájek M, Tišler Z et al (2021) The influence of long-term exposure of Mg–Al mixed oxide at ambient conditions on its transition to hydrotalcite: the long-term aging of Mg–Al mixed oxide. J Solid State Chem. https://doi.org/10.1016/j.jssc.2021.122556

Kots PA, Zabilska AV, Grigor'ev YV, Ivanova II (2019) Ethanol to butanol conversion over bifunctional zeotype catalysts containing palladium and zirconium. Pet Chem 59:925–934. https://doi.org/10.1134/S0965544119080097

Kuljiraseth J, Wangriya A, Malones JMC et al (2019) Synthesis and characterization of AMO LDH-derived mixed oxides with various Mg/Al ratios as acid–basic catalysts for esterification of benzoic acid with 2-ethylhexanol. Appl Catal B 243:415–427. https://doi.org/10.1016/j.apcatb.2018.10.073

León M, Díaz E, Ordóñez S (2011) Ethanol catalytic condensation over Mg–Al mixed oxides derived from hydrotalcites. Catal Today 164:436–442. https://doi.org/10.1016/j.cattod.2010.10.003

Lovón-Quintana JJ, Rodriguez-Guerrero JK, Valença PG (2017) Carbonate hydroxyapatite as a catalyst for ethanol conversion to hydrocarbon fuels. Appl Catal A Gen 542:136–145. https://doi.org/10.1016/j.apcata.2017.05.020

Lv Y, Li Y, Shen W (2013) Synthesis of Co3O4 nanotubes and their catalytic applications in CO oxidation. Catal Commun 42:116–120. https://doi.org/10.1016/j.catcom.2013.08.017

Ma W, Chen Y, Zhang W, Zhao W (2017) Performance and mechanism of Mg–Ca–Fe hydrotalcite-like compounds for fluoride removal from aqueous solution. J Fluor Chem 200:153–161. https://doi.org/10.1016/j.jfluchem.2017.06.012

Mališová M, Hájek M, Kocián D et al (2022) The influence of various anions in Mg–Al mixed oxides on presence of sodium ions in transesterification of oil. Fuel. https://doi.org/10.1016/j.fuel.2022.123781

Mandade P, Bakshi BR, Yadav GD (2016) Ethanol from Indian agro-industrial lignocellulosic biomass: an emergy evaluation. Clean Technol Environ Policy 18:2625–2634. https://doi.org/10.1007/s10098-016-1179-y

Mascal M (2012) Chemicals from biobutanol: technologies and markets. Biofuels, Bioprod Biorefin 8:483–493. https://doi.org/10.1002/BBB

Metzker G, Mora Vargas JA, de Lima LP et al (2021) First row transition metals on the ethanol Guerbet reaction: products distribution and structural behavior of mixed metal oxides as catalysts. Appl Catal A Gen 623:118272. https://doi.org/10.1016/j.apcata.2021.118272

Mück J, Kocík J, Hájek M et al (2021) Transition metals promoting Mg–Al mixed oxides for conversion of ethanol to butanol and other valuable products: reaction pathways. Appl Catal A Gen. https://doi.org/10.1016/j.apcata.2021.118380

Muttakin M, Mitra S, Thu K et al (2018) Theoretical framework to evaluate minimum desorption temperature for IUPAC classified adsorption isotherms. Int J Heat Mass Transf 122:795–805. https://doi.org/10.1016/j.ijheatmasstransfer.2018.01.107

Pavel OD, Tichit D, Marcu IC (2012) Acido–basic and catalytic properties of transition-metal containing Mg–Al hydrotalcites and their corresponding mixed oxides. Appl Clay Sci 61:52–58. https://doi.org/10.1016/j.clay.2012.03.006

Pérez A, Molina R, Moreno S (2014) Enhanced VOC oxidation over Ce/CoMgAl mixed oxides using a reconstruction method with EDTA precursors. Appl Catal A Gen 477:109–116. https://doi.org/10.1016/j.apcata.2014.03.011

Quesada J, Faba L, Díaz E, Ordóñez S (2018) Tuning the selectivities of Mg–Al mixed oxides for ethanol upgrading reactions through the presence of transition metals. Appl Catal A Gen 559:167–174. https://doi.org/10.1016/j.apcata.2018.04.022

Rechi Siqueira M, Micali Perrone O, Metzker G et al (2019) Highly selective 1-butanol obtained from ethanol catalyzed by mixed metal oxides: reaction optimization and catalyst structure behavior. Mol Catal. https://doi.org/10.1016/j.mcat.2019.110516

Smoláková L, Frolich K, Troppová I et al (2017) Determination of basic sites in Mg–Al mixed oxides by combination of TPD-CO_2 and CO_2 adsorption calorimetry: when the same basic sites are reported from both techniques? J Therm Anal Calorim 127:1921–1929. https://doi.org/10.1007/s10973-016-5851-6

Somma D, Lobkowicz H, Deason JP (2010) Growing America's fuel: an analysis of corn and cellulosic ethanol feasibility in the United States. Clean Technol Environ Policy 12:373–380. https://doi.org/10.1007/s10098-009-0234-3

Thommes M, Kaneko K, Neimark AV et al (2015) Physisorption of gases, with special reference to the evaluation of surface area and pore size distribution (IUPAC technical report). Pure Appl Chem 87:1051–1069. https://doi.org/10.1515/pac-2014-1117

Veibel S, Nielsen JI (1967) On the mechanism of the Guerbet reaction. Tetrahedron 23:1723–1733. https://doi.org/10.1016/S0040-4020(01)82571-0

Volli V, Purkait MK (2016) Preparation and characterization of hydrotalcite-like materials from flyash for transesterification. Clean Technol Environ Policy 18:529–540. https://doi.org/10.1007/s10098-015-1036-4

Wingad RL, Bergström EJE, Everett M et al (2016) Catalytic conversion of methanol/ethanol to isobutanol-a highly selective route to an advanced biofuel. Chem Commun 52:5202–5204. https://doi.org/10.1039/c6cc01599a

Wu X, Fang G, Liang Z et al (2017) Catalytic upgrading of ethanol to n-butanol over M-CeO2/AC (M = Cu, Fe Co, Ni and Pd) catalysts. Catal Commun 100:15–18. https://doi.org/10.1016/j.catcom.2017.06.016

Xu G, Lammens T, Liu Q et al (2014) Direct self-condensation of bio-alcohols in the aqueous phase. Green Chem 16:3971–3977. https://doi.org/10.1039/c4gc00510d

Zawadzki M, Walerczyk W, López-Suárez FE et al (2011) $CoAl_2O_4$ spinel catalyst for soot combustion with NO_x/O_2. Catal Commun 12:1238–1241. https://doi.org/10.1016/j.catcom.2011.04.021

Zgheib N, Takache H (2021) Recycling of used lubricating oil by solvent extraction: experimental results, aspen Plus simulation and feasibility study. Clean Technol Environ Policy 23:65–76. https://doi.org/10.1007/s10098-020-01893-0

Zhou M, Zeng Z, Zhu H et al (2014) Aqueous-phase catalytic hydrogenation of furfural to cyclopentanol over Cu–Mg–Al hydrotalcites derived catalysts: model reaction for upgrading of bio-oil. J Energy Chem 23:91–96. https://doi.org/10.1016/S2095-4956(14)60109-

Authors and Affiliations

Karel Frolich[1] · Jan Malina[1] · Martin Hájek[1] · Jáchym Mück[1] · Jaroslav Kocík[2]

✉ Jan Malina
jan.malina@student.upce.cz

[1] Department of Physical Chemistry, Faculty of Chemical Technology, University of Pardubice, Studentská 95, 532 10 Pardubice, Czech Republic

[2] ORLEN UniCRE a.s, Revoluční 84, 1521, 400 01 Ústí Nad Labem, Czech Republic